

## *Supplementary Information*

# **Multiple rotational rates in a guest-loaded, amphidynamic zirconia metal-organic framework**

Aaron Torres-Huerta,<sup>1</sup> Dazaet Galicia-Badillo<sup>1</sup> Andrés Aguilar-Granda,<sup>1†</sup> Jacob T. Bryant,<sup>2</sup>  
Fernando J. Uribe-Romo,<sup>2\*</sup> and Braulio Rodríguez-Molina<sup>1\*</sup>

<sup>1</sup>Instituto de Química, Universidad Nacional Autónoma de México, Circuito Exterior,  
Ciudad Universitaria, 04510, Ciudad de México, México.

<sup>2</sup>Department of Chemistry and Renewable Energy and Chemical Transformations Cluster,  
University of Central Florida, 4111 Libra Drive, Room 251 PSB, 32816-2366, Orlando,  
Florida, United States.

Present Address: †Department of Chemistry, University of Toronto, Toronto, ON M5S  
3H6, Canada.

[\\*fernando@ucf.edu](mailto:*fernando@ucf.edu)

[\\*brodriguez@iquimica.unam.mx](mailto:*brodriguez@iquimica.unam.mx)

## Contents

<b>1. Experimental section</b> .....	<b>S6</b>
2.1 Organic linkers synthesis .....	S6
2.2 Synthesis and characterization of PIZOF-2, and its deuterated analogues PIZOF-2d <sub>4</sub> , and PIZOF-2d <sub>8</sub> .....	S8
2.3 Synthesis of TCNQ@PIZOF-2 materials .....	S14
2.4 Determination of TCNQ loaded into MOF samples .....	S19
2.5 <sup>1</sup> H RMN and solid-state NMR <sup>13</sup> C CPMAS spectra .....	S20

## Table of Schemes and Figures

**Scheme S1:** Synthesis route of the 1,4-diethynylbenzene (**3**), 1,4-diethynylbenzene-d<sub>4</sub> (**3-d<sub>4</sub>**) and methyl-4-iodobenzoate-d<sub>4</sub> (**5-d<sub>4</sub>**). .....

S6

**Scheme S2:** Synthesis route of **PEPEP** linker and its deuterated derivatives (**PEPEP-d<sub>4</sub>**, and **PEPEP-d<sub>8</sub>**) .....

S6

**Figure S1:** Experimental PXRD patterns of **PIZOF-2** and calculated PXRD patterns of interpenetrated and non-interpenetrated crystalline phases. ....

S9

**Figure S2:** Rietveld plot of **PEPEP-PIZOF-2** natural abundance. Blue marks = observed, green trace = refined, teal = difference, red trace = background. ....

S10

**Figure S3:** Rietveld plot of **PEPEP-PIZOF-2d<sub>4</sub>**. Blue marks = observed, green trace = refined, teal = difference, red trace = background. ....

S10

**Figure S4:** Rietveld plot of **PEPEP-PIZOF-2d<sub>8</sub>**. Blue marks = observed, green trace = refined, teal = difference, red trace = background. ....

S11

**Figure S5:** IR spectra of the compounds **PIZOF-2**, **PIZOF-2d<sub>4</sub>** and **PIZOF-2d<sub>8</sub>**. ....

S12

**Figure S6:** Solid state NMR <sup>13</sup>C CPMAS spectra of compounds **PIZOF-2**, **PIZOF-2d<sub>4</sub>** and **PIZOF-2d<sub>8</sub>**. ....

S13

**Figure S7:** a) Fragment of the crystal structure of **PIZOF-2** highlighting its interpenetrated lattice; b) The distances among four different linkers coordinated to the same cluster. ....

S14

<b>Figure S8:</b> a) Solid state NMR $^{13}\text{C}$ CPMAS spectroscopy of the guest (TCNQ), the <b>PIZOF-2</b> and the new <b>TCNQ@PIZOF-2</b> system. b) Comparative analysis by powder X-ray diffraction; c) Electron Paramagnetic Resonance spectroscopy with the signal for the CT interaction and d) Fluorescence quenching of the <b>TCNQ@PIZOF-2</b> system. ....	S15
<b>Figure S9:</b> Le Bail fit of the PXRD pattern of <b>TCNQ@PIZOF-2</b> . ....	S15
<b>Figure S10:</b> IR spectra of the compounds <b>TCNQ@PIZOF-2d<sub>8</sub></b> , <b>TCNQ@PIZOF-2d<sub>4</sub></b> and <b>TCNQ@PIZOF-2</b> . ....	S16
<b>Figure S11:</b> Solid state NMR $^{13}\text{C}$ CPMAS spectra of <b>TCNQ@PIZOF-2d<sub>8</sub></b> , <b>TCNQ@PIZOF-2d<sub>4</sub></b> and <b>TCNQ@PIZOF-2</b> . ....	S16
<b>Figure S12:</b> Evolution of the $^{13}\text{C}$ CPMAS spectra in <b>TCNQ@PIZOF-2d<sub>4</sub></b> with different infiltration times. ....	S17
<b>Figure S13:</b> PXRD diffraction patterns of <b>TCNQ@PIZOF-2d<sub>4</sub></b> varying the infiltration times. ....	S17
<b>Figure S14:</b> Differential scanning calorimetry (blue line) and thermogravimetric analyses (black line) trace of compound <b>PIZOF-2</b> . ....	S18
<b>Figure S15:</b> Differential scanning calorimetry (blue line) and thermogravimetric analyses (black line) trace of compound <b>TCNQ@PIZOF-2</b> . ....	S18
<b>Figure S16:</b> a) UV-vis spectra of TCNQ with different concentrations in the range from 0.5 mM to 2.5 mM. b) Calibration plot of the absorbance ( $\lambda_{\text{max}} = 400$ nm) vs TCNQ concentration with a linear fit (blue line). c) UV-vis spectra of <b>TCNQ@PIZOF-2d<sub>4</sub></b> with infiltration times of 6 h, 24 h, 48 h, and 72 h. d) Relative concentration plot of TCNQ loaded into <b>PIZOF-2d<sub>4</sub></b> (Taking as 100 % the intensity of the absorbance at 400 nm of the sample with an infiltration time of 72 h). ....	S19
<b>Figure S17:</b> $^1\text{H}$ NMR spectrum of compound <b>Me-PEPEP</b> (300 MHz, $\text{CDCl}_3$ ). ....	S20
<b>Figure S18:</b> $^1\text{H}$ NMR spectrum of compound <b>PEPEP</b> (300 MHz, $\text{DMSO-d}_6$ ). ....	S21
<b>Figure S19:</b> $^1\text{H}$ NMR spectrum of compound <b>Me-PEPEP-d<sub>4</sub></b> (300 MHz, $\text{CDCl}_3$ ). ....	S21
<b>Figure S20:</b> $^1\text{H}$ NMR spectrum of compound <b>PEPEP-d<sub>4</sub></b> (300 MHz, $\text{DMSO-d}_6$ ). ....	S22
<b>Figure S21:</b> $^1\text{H}$ NMR spectrum of compound <b>Me-PEPEP-d<sub>8</sub></b> (300 MHz, $\text{CDCl}_3$ ). ....	S22
<b>Figure S22:</b> $^1\text{H}$ NMR spectrum of compound <b>PEPEP-d<sub>8</sub></b> (300 MHz, $\text{DMSO-d}_6$ ). ....	S23
<b>Figure S23:</b> Solid-state NMR $^{13}\text{C}$ CPMAS spectrum of TCNQ. ....	S23
<b>Figure S24:</b> Solid-state NMR $^{13}\text{C}$ CPMAS spectrum of <b>PIZOF-2</b> . ....	S24

<b>Figure S25:</b> Solid-state NMR $^{13}\text{C}$ CPMAS spectrum of <b>PIZOF-2d<sub>4</sub></b> .....	S24
<b>Figure S26:</b> Solid-state NMR $^{13}\text{C}$ CPMAS spectrum of <b>PIZOF-2d<sub>8</sub></b> .....	S25
<b>Figure S27:</b> Solid-state NMR $^{13}\text{C}$ CPMAS spectrum of <b>TCNQ@PIZOF-2</b> .....	S25
<b>Figure S28:</b> Solid-state NMR $^{13}\text{C}$ CPMAS spectrum of <b>TCNQ@PIZOF-2d<sub>4</sub></b> .....	S26
<b>Figure S29:</b> Solid-state NMR $^{13}\text{C}$ CPMAS spectrum of <b>TCNQ@PIZOF-2d<sub>8</sub></b> .....	S26

## 1. Materials and methods

**Synthesis.** All reagents were purchased from Sigma-Aldrich and used without further purification. THF was dried prior to use by distillation over Na/benzophenone. Flash column chromatography was performed using silica gel Aldrich 230-400 mesh. Reactions were monitored by TLC on silica gel plates 60 F254 (Merck) and spots were detected by UV-absorption.  $^1\text{H}$  and  $^{13}\text{C}$  NMR data for all compounds were recorded at ambient temperature using Bruker Fourier300 and Jeol Eclipse 300 with cryoprobe spectrometers. FT-IR spectra were recorded with Bruker ATR in the  $450\text{--}4000\text{ cm}^{-1}$  range. Melting points were determined using Fisher Johns melting point apparatus. HRMS (High Resolution Mass Spectroscopy) were obtained in a coupled liquid-chromatography mass-spectrometry system with single quadrupole and time-of-flight (HPLC-EM-SQ-TOF); Agilent Tech, model G6530BA. Differential scanning calorimetry and thermogravimetric analyses were carried out on a DSC analyzer Netzsch STA 449 F3 Jupiter. Measurements were collected from 25 to 550 °C with a heating rate of 10 °C/min under an air atmosphere. PXRD measurements were carried out at room temperature, and the data were collected in the range of  $2\theta = 5\text{--}30^\circ$ , using  $\text{Cu-K}\alpha_1 = 1.5418\text{ \AA}$  radiation.

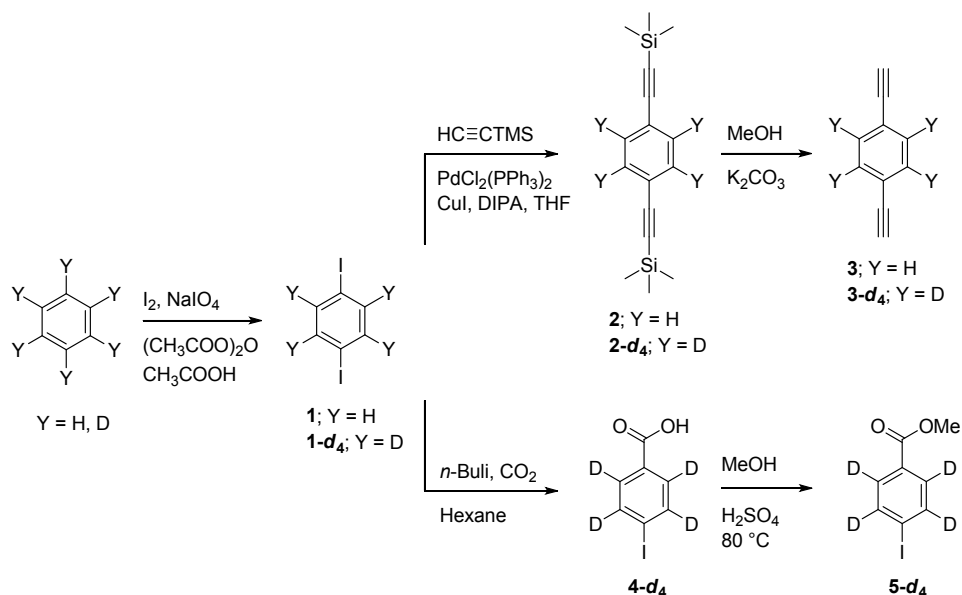
**Solid state NMR.**  $^2\text{H}$  spin-echo experiments were performed on a Bruker Ascend at 76.78 MHz (deuterium resonance frequency) with a  $90^\circ$  pulse of 8.0  $\mu\text{s}$ . An echo delay of 50  $\mu\text{s}$  was used after the refocusing delay of 46  $\mu\text{s}$ , and the recycle delay between pulses was 2 s. All spectra in this work were obtained using a line broadening of 2.0 kHz in the data processing. Simulated  $^2\text{H}$  NMR spectra for a  $180^\circ$  jumps model was performed by NMR Web Lab (6.6.3).<sup>1</sup> A 180 kHz C- $^2\text{H}$  QCC was used, with a  $60^\circ$  cone angle and 50  $\mu\text{s}$  pulse delay. In the case of **PIZOF-2d<sub>4</sub>** samples, oscillations with  $\pm 45^\circ$  were added.

**Powder X-ray Diffraction.** Rietveld refinements were performed in GSAS-II<sup>2</sup> with the experimental diffractograms, and the crystal model obtained from Cambridge Structural Database (CSD code: OXOLAP, space group Fd-3m). Refinements were performed using a Thomson-Cox-Hasting modified pseudo-Voigt function with 6 terms with Finger-Cox-Jephcoat peak asymmetry with 1 parameter. The background was initially hand fit to a 6th order Shifted Chebyshev polynomial. The profile was initially calculated using the LeBail routine (Peakfit) with manually picked peaks, refining first the Gaussian and then the Lorentzian components, followed by asymmetry and background, observing convergent refinements. Following LeBail fit, Rietveld routine with extraction of the structure factors (Fobs) was then used refining the scale factor, unit cell parameters, zero shift and LP function, followed by the background function, the crystallite size and strain broadening, transparency and extinction. A preferred orientation correction was added to the refinements using a 2nd order spherical harmonic function. Isotropic atomic displacement parameters (Uiso) of all non-hydrogen atoms were refined with constraints (constraining all the chemically equivalent atoms). Final refinements included all parameters, which were refined iteratively until convergent refinements were obtained. Fobs were extracted, and a crystallographic information file (CIF) was generated. In all samples, the presence only the interpenetrated phase was obtained and the non-interpenetrated phase<sup>3</sup> with a characteristic diffraction peak at  $2\theta = 4.43^\circ$ ;  $h,k,l = 2,0,0$  was ruled out (Figure S1).

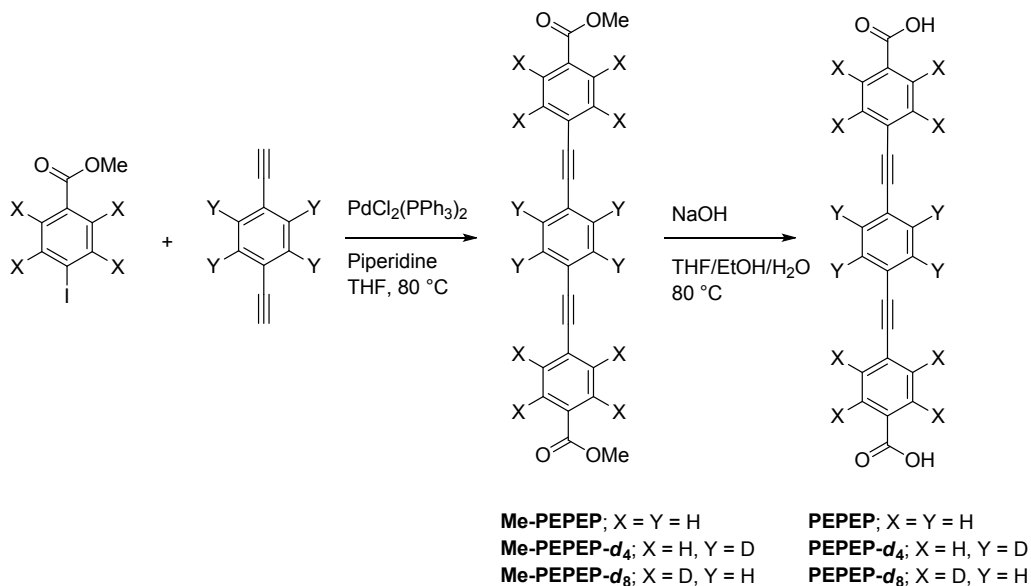
## 1. Experimental section

### 2.1 Organic linkers synthesis

The compounds **3**, **3-*d*<sub>4</sub>** and **5-*d*<sub>4</sub>** were synthesized according to literature procedures.<sup>4</sup>



**Scheme S1:** Synthesis route of the 1,4-diethynylbenzene (**3**), 1,4-diethynylbenzene-*d*<sub>4</sub> (**3-*d*<sub>4</sub>**) and methyl-4-iodobenzoate-*d*<sub>4</sub> (**5-*d*<sub>4</sub>**).



**Scheme S2:** Synthesis route of **PEPEP** linker and its deuterated derivatives (**PEPEP-*d*<sub>4</sub>** and **PEPEP-*d*<sub>8</sub>**).

**Me-PEPEP:** In a two-neck round bottom flask, methyl 4-iodobenzoate (1.000 g, 3.816 mmol), 1,4-diethynylbenzene (0.240 g, 1.908 mmol), PdCl<sub>2</sub>(PPh<sub>3</sub>)<sub>2</sub> (0.214 g, 0.305 mmol),

diisopropylamine (1 mL) and dry THF (12 mL) were dissolved and refluxed overnight under nitrogen atmosphere. Afterwards, the mixture was quenched with a saturated solution of  $\text{NH}_4\text{Cl}$  (50 mL). Then, the precipitated was filtered and washed with water, hexane, and dichloromethane to afford a yellowish solid. Yield: 73 % (0.550 g, 1.394 mmol). FT-IR (ATR)  $\tilde{\nu}$  3033 (w), 2956 (w), 2837 (w), 1710 (s), 1637 (s), 1575, (m), 1549 (w), 1539 (w), 1533 (w), 1499 (w), 1430 (m), 1410 (m), 1321 (m), 1293 (m), 1229 (m), 1121 (w), 1066 (s), 944 (w), 912 (m), 839 (s), 817 (m), 686 (s), 614 (m), 538 (m)  $\text{cm}^{-1}$ .  $^1\text{H}$  NMR (300 MHz,  $\text{CDCl}_3$ )  $\delta$  3.93 (s, 6H), 7.54 (s, 4H), 7.61 (d,  $^3J = 8.6$  Hz, 4H), 8.04 (d,  $^3J = 8.5$  Hz, 4H). HRMS (HPLC-EM-SQ-TOF)  $m/z$  [ $\text{C}_{26}\text{H}_{19}\text{O}_4$ ] $^+$  calcd. 395.1283 found 395.1278; error 1.26 ppm.

**Me-PEPEP- $d_4$** : Compound **Me-PEPEP- $d_4$**  was obtained following the same procedure as described for **Me-PEPEP**, using 1,4-diethynylbenzene- $d_4$  (0.248 g, 1.908 mmol), instead of 1,4-diethynylbenzene- $d_4$ . Yield: 76 % (0.577 g, 1.448 mmol). FT-IR (ATR)  $\tilde{\nu}$  3128 (w), 3021 (w), 2956 (w), 2843 (w), 1712 (s), 1641 (m), 1570, (m), 1547 (m), 1534 (w), 1532 (w), 1499 (w), 1433 (m), 1413 (m), 1397 (m), 1314 (s), 1288 (m), 1275 (w), 1232 (s), 1118 (w), 1108 (w), 1072 (s), 1014 (w), 945 (w), 912 (m), 861 (w), 834 (s), 821 (s), 683 (s), 650 (w), 612 (w), 595 (w), 544 (w)  $\text{cm}^{-1}$ .  $^1\text{H}$  NMR (300 MHz,  $\text{CDCl}_3$ )  $\delta$  3.94 (s, 6H), 7.61 (d,  $^3J = 8.6$  Hz, 4H), 8.05 (d,  $^3J = 8.6$  Hz, 4H). HRMS (HPLC-EM-SQ-TOF)  $m/z$  [ $\text{C}_{26}\text{H}_{15}\text{D}_4\text{O}_4$ ] $^+$  calcd. 399.1534 found 399.1529; error 1.25 ppm.

**Me-PEPEP- $d_8$** : Compound **Me-PEPEP- $d_8$**  was obtained following the same procedure as described for **Me-PEPEP**, using methyl-4-iodobenzoate- $d_4$  (0.200 g, 0.751 mmol), instead of methyl-4-iodobenzoate. Yield: 52 % (0.078 g, 0.194 mmol). FT-IR (ATR)  $\tilde{\nu}$  3133 (w), 3033 (w), 2956 (w), 1711 (s), 1644 (m), 1572, (m), 1550 (w), 1534 (w), 1438 (m), 1405 (m), 1321 (s), 1291 (s), 1227 (s), 1120 (w), 1072 (s), 1011 (w), 945 (w), 910 (m), 861 (w), 839 (s), 818 (m), 682 (s), 615 (m), 590 (w), 539 (m)  $\text{cm}^{-1}$ .  $^1\text{H}$  NMR (300 MHz,  $\text{CDCl}_3$ )  $\delta$  3.93 (s, 6H), 7.54 (s, 4H).

**PEPEP**: In a two-neck round bottom flask, **Me-PEPEP** (0.500 g, 1.267 mmol), NaOH (0.507 mg, 12.677 mmol) in a mixture of THF (12 mL), EtOH (6 mL),  $\text{H}_2\text{O}$  (6 mL) were refluxed overnight at 80  $^\circ\text{C}$ . Afterwards, the reaction solution was diluted with water (50 mL) and acidified by the addition of hydrochloric acid. The final product was filtered and

washed with water, acetone, and dichloromethane to afford a yellowish solid. Yield: 92 % (0.427 g, 1.165 mmol). FT-IR (ATR)  $\tilde{\nu}$  3411 (w), 3075 (w), 3039 (w), 2966 (m), 2841 (m), 2622 (w), 2545 (w) 1675 (s), 1636 (m), 1555 (m), 1516 (w), 1488 (m), 1375 (w), 1310 (m), 1299 (m), 1271 (m), 1207 (m), 1100 (w), 1066 (w), 952 (w), 899 (m), 859 (w) 827 (s), 809 (w), 768 (w), 686 (s), 646 (w), 606 (w), 547 (m)  $\text{cm}^{-1}$ .  $^1\text{H}$  NMR (300 MHz, DMSO- $d_6$ )  $\delta$  7.67 (s, 4H) 7.71 (d,  $^3J = 8.4$  Hz, 4H), 8.00 (d,  $^3J = 8.4$  Hz, 4H). HRMS (HPLC-EM-SQ-TOF)  $m/z$  [ $\text{C}_{24}\text{H}_{13}\text{O}_4$ ] $^-$  calcd. 365.0814 found 365.0803; error 3.00 ppm.

**PEPEP- $d_4$** : Compound **PEPEP- $d_4$**  was obtained following the same procedure as described for **PEPEP**. Yield: 90 % (0.418 g, 1.129 mmol). FT-IR (ATR)  $\tilde{\nu}$  3070 (w), 3017 (w), 2960 (m), 2839 (m), 2630 (w), 2541 (w) 1677 (s), 1635 (m), 1555 (m), 1516 (w), 1501 (w), 1478 (m), 1375 (w), 1310 (m), 1299 (m), 1262 (m), 1201 (w), 1065 (w), 948 (w), 891 (m), 873 (w) 821 (s), 809 (w), 766 (w), 755 (w), 687 (s), 653 (w), 613 (w)  $\text{cm}^{-1}$ .  $^1\text{H}$  NMR (300 MHz (DMSO- $d_6$ )  $\delta$  7.70 (d,  $^3J = 8.1$  Hz, 4H), 8.00 (d,  $^3J = 8.2$  Hz, 4H). HRMS (HPLC-EM-SQ-TOF)  $m/z$  [ $\text{C}_{24}\text{H}_9\text{D}_4\text{O}_4$ ] $^-$  calcd. 369.1065 found 369.1063; error 0.54 ppm.

**PEPEP- $d_8$** : Compound **PEPEP- $d_8$**  was obtained following the same procedure as described for **PEPEP**. Yield: 94 % (0.61 g, 0.163 mmol). FT-IR (ATR)  $\tilde{\nu}$  3046 (w), 2931 (m), 2853 (m), 2622 (w), 2537 (w) 1679 (s), 1638 (m), 1573 (m), 1530 (w), 1414 (m), 1391 (w), 1326 (s), 1299 (w), 1253 (w), 1218 (m), 1106 (w), 1072 (w), 944 (w), 921 (w), 864 (w), 841 (w), 806 (w), 794 (w), 752 (w), 683 (s), 606 (w), 590 (w), 555 (m), 517 (w)  $\text{cm}^{-1}$ .  $^1\text{H}$  NMR (300 MHz, DMSO- $d_6$ )  $\delta$  7.67 (s, 4H). HRMS (HPLC-EM-SQ-TOF)  $m/z$  [ $\text{C}_{24}\text{H}_5\text{D}_8\text{O}_4$ ] $^-$  calcd. 373.1316 found 373.1278; error 10.18 ppm.

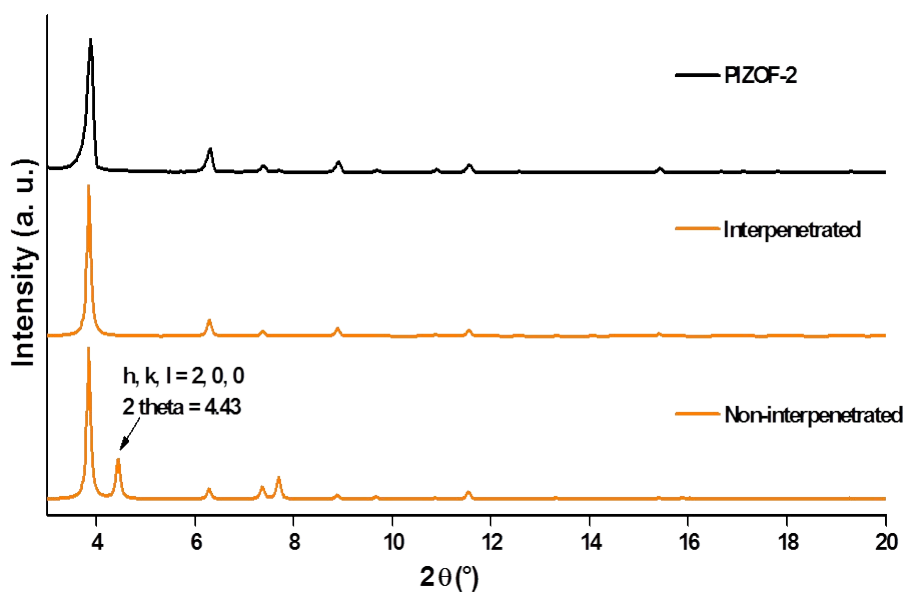
## 2.2 Synthesis and characterization of PIZOF-2, and its deuterated analogues PIZOF- $2d_4$ , and PIZOF- $2d_8$

The MOFs **PIZOF-2**, **PIZOF- $2d_4$** , and **PIZOF- $d_8$**  were synthesized according to literature procedures with slight modifications.<sup>5</sup>

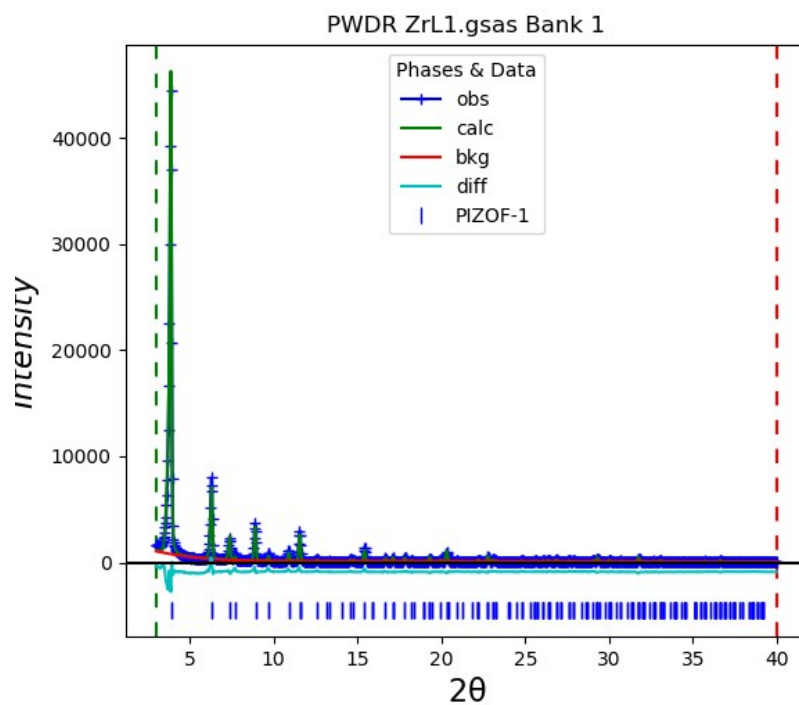
**PIZOF-2**: L-proline (0.130 g, 1.13 mmol), zirconium chloride (0.052 g, 0.22 mmol), **PEPEP** (0.082 g, 0.22 mmol, 1 eq), and DMF (10 mL) were added to a 20 ml capped vial and sonicated for 15 minutes. Afterwards, concentrated HCl (0.02 ml) was added and the suspension was sonicated for a further 15 minutes before being placed in the oven at 120

°C for 24 hours. The bulk material was filtered and washed with DMF, acetone, and dichloromethane. For activation: the powder sample was added to 20 mL capped vial and left to stand in DMF for 24 h. Then, the solvent was exchanged by acetone and the sample was incubated in this solvent for a further 24 h. Finally, acetone was exchanged for CH<sub>2</sub>Cl<sub>2</sub>, and the sample was incubated in this solvent for 3 days. During this incubation time the CH<sub>2</sub>Cl<sub>2</sub> was replaced three times by fresh solvent. The sample was isolated by filtration and dried under vacuum for 24 hours. Yield [Zr<sub>6</sub>O<sub>4</sub>(OH)<sub>4</sub>(L1)<sub>6</sub>]<sub>n</sub>: 86 % (0.090 g, 0.032 mmol).

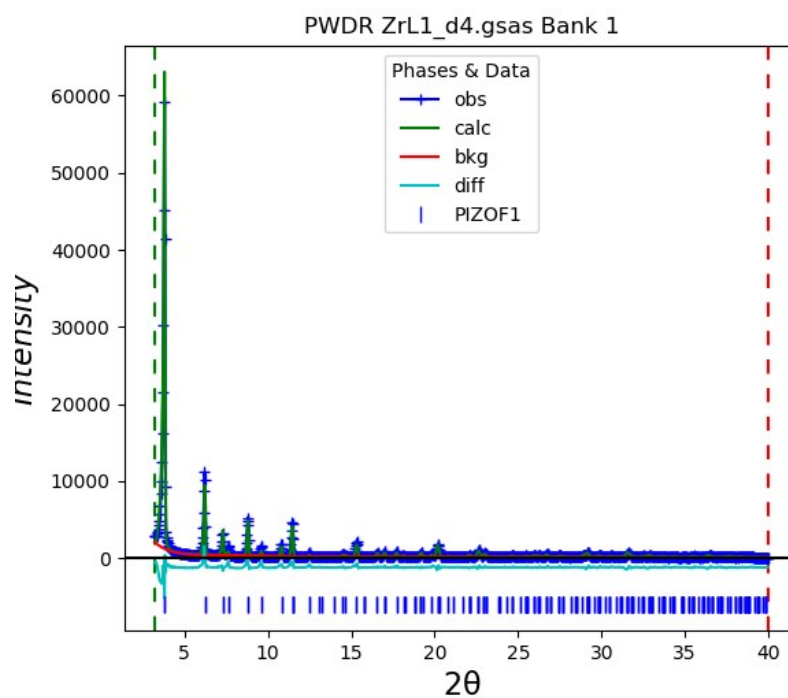
**PIZOF-2d<sub>4</sub>** and **PIZOF-2d<sub>8</sub>** was obtained following the same procedure as describe for **PIZOF-2**.



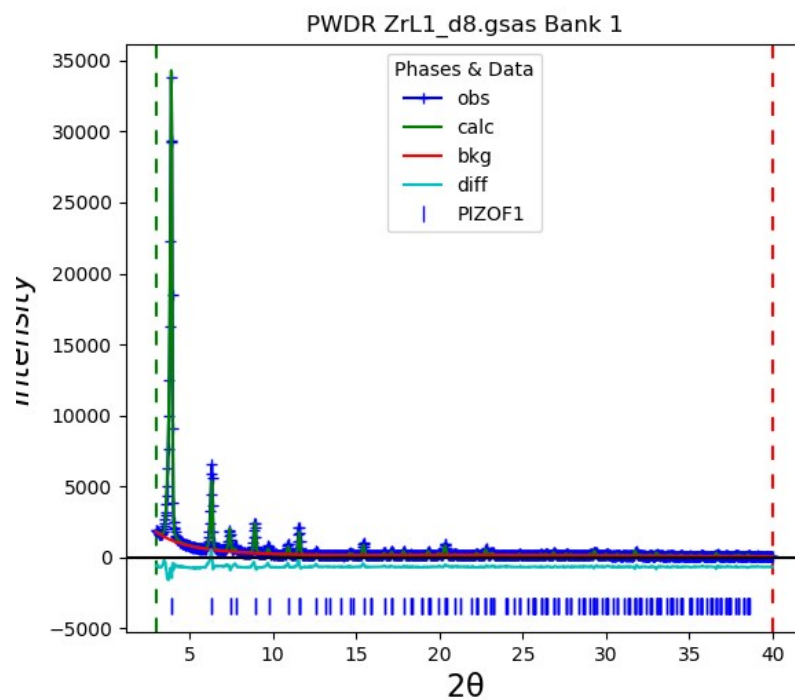
**Figure S1:** Experimental PXRD patterns of **PIZOF-2** and calculated PXRD patterns of interpenetrated and non-interpenetrated crystalline phases.



**Figure S2.** Rietveld plot of **PEPEP-PIZOF-2** natural abundance. Blue marks = observed, green trace = refined, teal = difference, red trace = background.



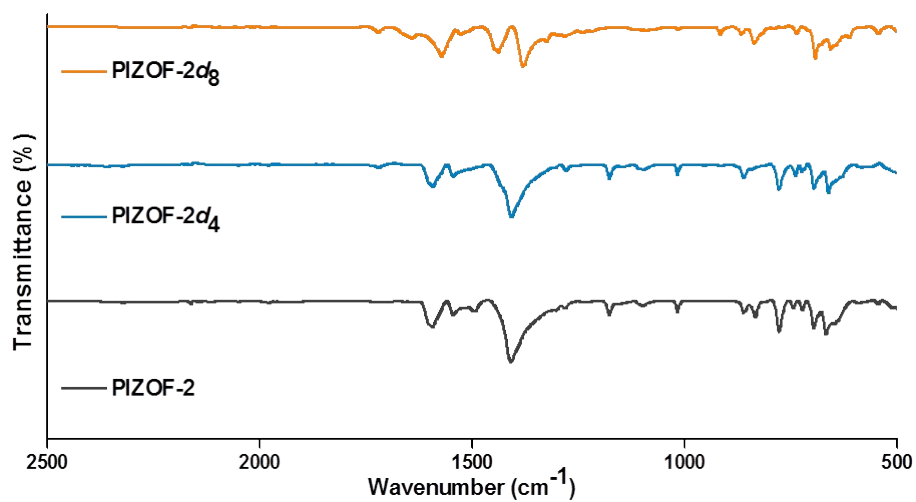
**Figure S3.** Rietveld plot of **PEPEP-PIZOF-2d<sub>4</sub>**. Blue marks = observed, green trace = refined, teal = difference, red trace = background.



**Figure S4.** Rietveld plot of **PEPEP-PIZOF-2d<sub>8</sub>**. Blue marks = observed, green trace = refined, teal = difference, red trace = background.

**Table S1.** Crystallographic information from Rietveld Refinement.

Name	PEPEP-PIZOF-2	PEPEP-PIZOF-2 <i>d</i> <sub>4</sub>	PEPEP-PIZOF-2 <i>d</i> <sub>8</sub>
Asymmetric composition unit	C <sub>48</sub> O <sub>10.667</sub> Zr <sub>2</sub>	C <sub>48</sub> O <sub>10.667</sub> Zr <sub>2</sub>	C <sub>48</sub> O <sub>10.667</sub> Zr <sub>2</sub>
Formula weight (g mol <sup>-1</sup> )	929.62	929.62	929.62
Temperature (K)	300	300	300
Z	48	48	48
Crystal system	cubic	cubic	cubic
Space Group	<i>Fd-3m</i> (No. 227)	<i>Fd-3m</i> (No. 227)	<i>Fd-3m</i> (No. 227)
<i>a</i> (Å)	39.949(10)	41.164(15)	40.346(11)
<i>V</i> (Å <sup>3</sup> )	63750(50)	69750(80)	6567(50)
Number of independent atoms	13	13	13
Observed reflections	164	173	155
Number of data points	2636	2523	2636
Max <i>d</i> -spacing resolution (Å)	23.064	23.766	23.294
Min <i>d</i> -spacing resolution (Å)	2.036	2.319	2.361
Refined parameters (total)	35	21	24
<i>R</i> <sub>p</sub> (%)	10.017	13.054	8.668
<i>wR</i> <sub>p</sub> (%)	14.148	17.313	12.20
<i>R</i> <sub>B</sub> (%)	11.222	12.694	7.976
GOF (χ <sup>2</sup> )	3.103	4.434	2.706

**Figure S5:** IR spectra of the compounds **PIZOF-2**, **PIZOF-2*d*<sub>4</sub>** and **PIZOF-2*d*<sub>8</sub>**.

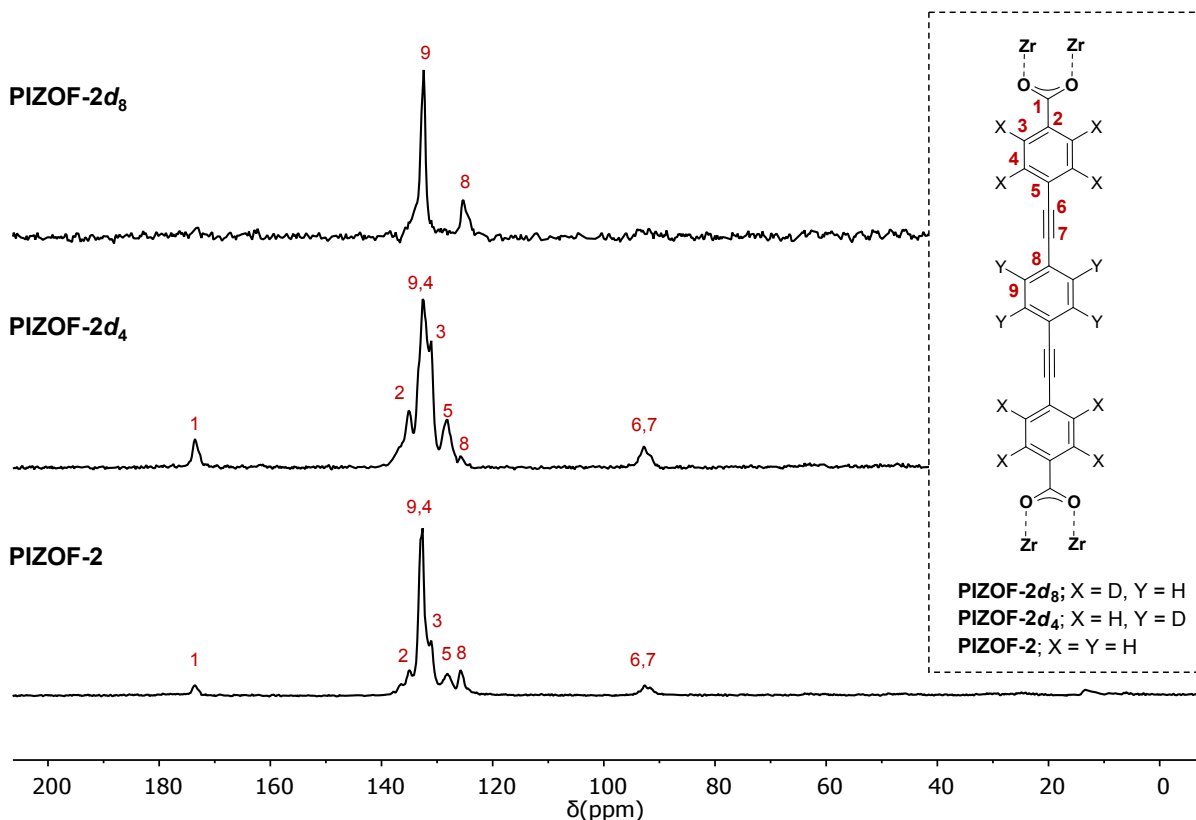


**Figure S6:** Solid state NMR  $^{13}\text{C}$  CPMAS spectra of compounds **PIZOF-2**, **PIZOF-2d<sub>4</sub>** and **PIZOF-2d<sub>8</sub>**.

**SCXRD:** The crystalline structure of **PIZOF-2** was first reported by Cordova et al.<sup>6</sup> as a cubic *Fd3-m* space group with  $a = 39.8116(7)$  Å. The MOF **PIZOF-2** is constituted by the  $[\text{Zr}_6\text{O}_4(\text{OH})_4(\text{L1})_6]_n$  unit, where the cluster  $\text{Zr}_6\text{O}_4(\text{OH})_4$  is connected to twelve **PEPEP** linkers affording a 2-fold interpenetrated network.

In the other hand, the rotational dynamics observed in **PIZOF-2d<sub>4</sub>** and **PIZOF-2d<sub>8</sub>** was supported by the analysis of the molecular structure of **PIZOF-2**. The crystalline structure of the MOF **PIZOF-2** showed a considerable separation between its linkers despite its interpenetration (Figure S7). This is clearly seen in the distance between the hydrogen H(9) of the central aromatic ring with the hydrogen atoms H(3) and H(4) from the neighboring aromatic rings, with distances of 3.07 Å and 2.90 Å, respectively (Figure S7a). Detailed inspection of the aromatic rings closer to the cluster  $\text{Zr}_6\text{O}_4(\text{OH})_4$  also showed a significant separation between their aromatic rings with distances of 6.53 Å and 8.03 Å (Figure S7b).

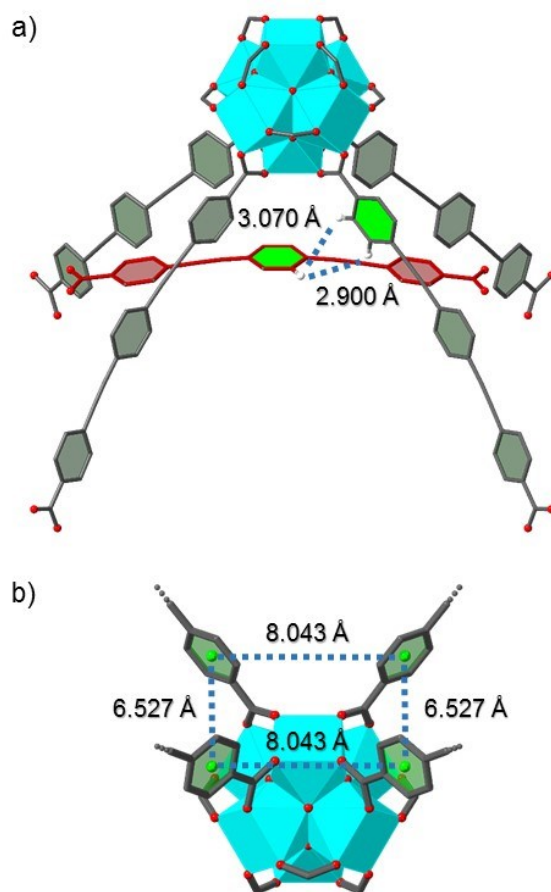


**Figure S7:** a) Fragment of the crystal structure of **PIZOF-2** highlighting its interpenetrated lattice; b) The distances among four different linkers coordinated to the same cluster.

### 2.3 Synthesis of TCNQ@PIZOF-2 materials

**TCNQ@PIZOF-2:** **PIZOF-2** (150 mg, 0.052 mmol), TCNQ (0.204g 0.999 mmol) in  $\text{CH}_2\text{Cl}_2$  (20 mL) were added to a 50 mL capped vial and left to stand for 72 hours at room temperature. The powder was filtered and washed with 6 ml of DCM and dried under vacuum for 1 hour. A similar procedure was followed to generate the samples **TCNQ@PIZOF-2<sub>d4</sub>**, **TCNQ@PIZOF-2<sub>d8</sub>**.

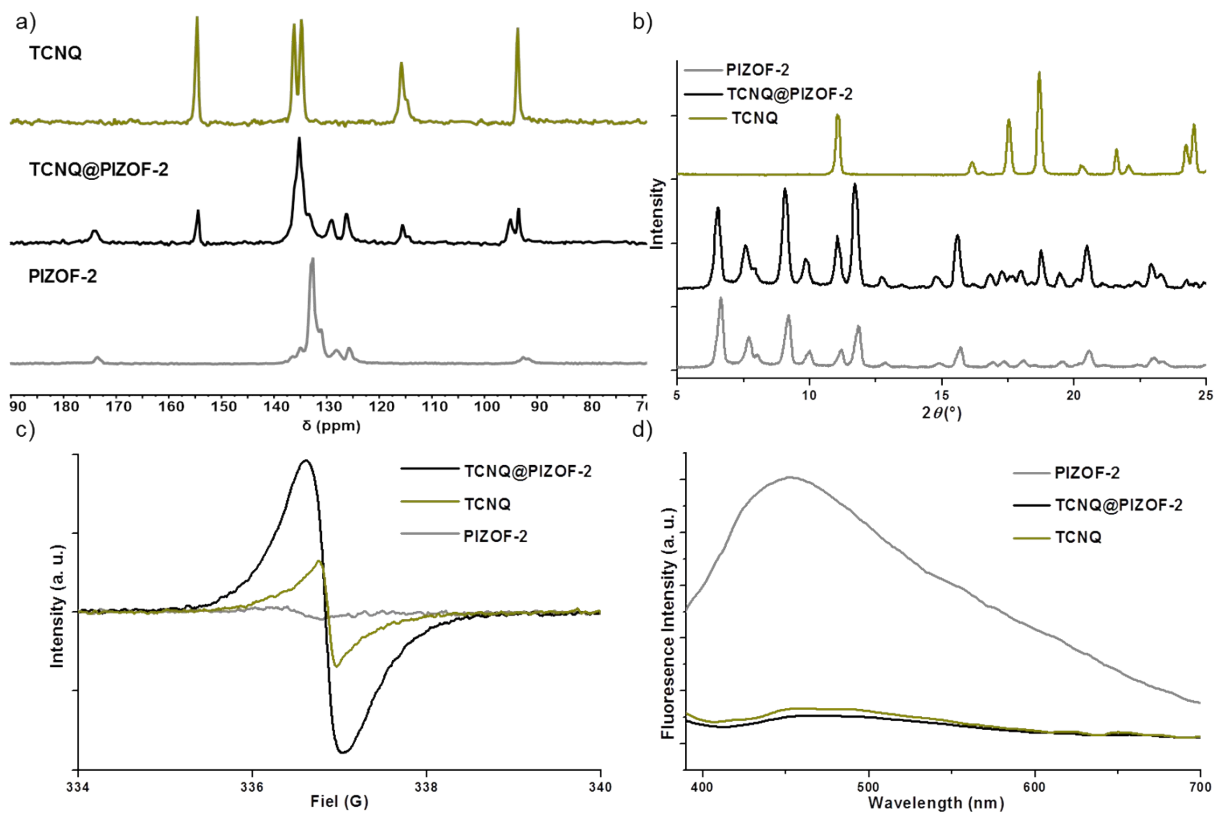


**Figure S8:** a) Solid state NMR  $^{13}\text{C}$  CPMAS spectroscopy of the guest (TCNQ), the **PIZOF-2** and the new **TCNQ@PIZOF-2** system. b) Comparative analysis by powder X-ray diffraction; c) Electron Paramagnetic Resonance spectroscopy with the signal for the CT interaction and d) Fluorescence quenching of the **TCNQ@PIZOF-2** system.

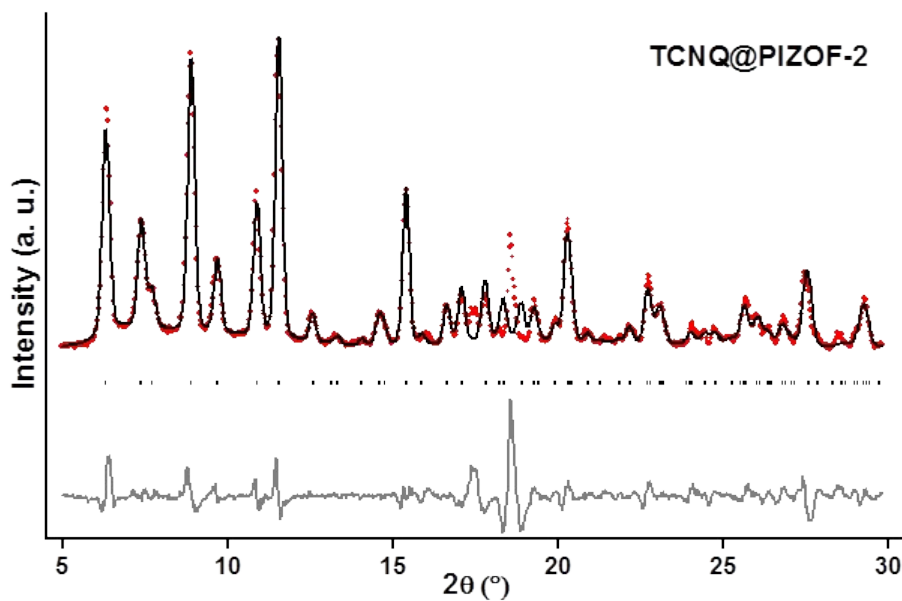


**Figure S9:** Le Bail fit of the PXRD pattern of **TCNQ@PIZOF-2**.

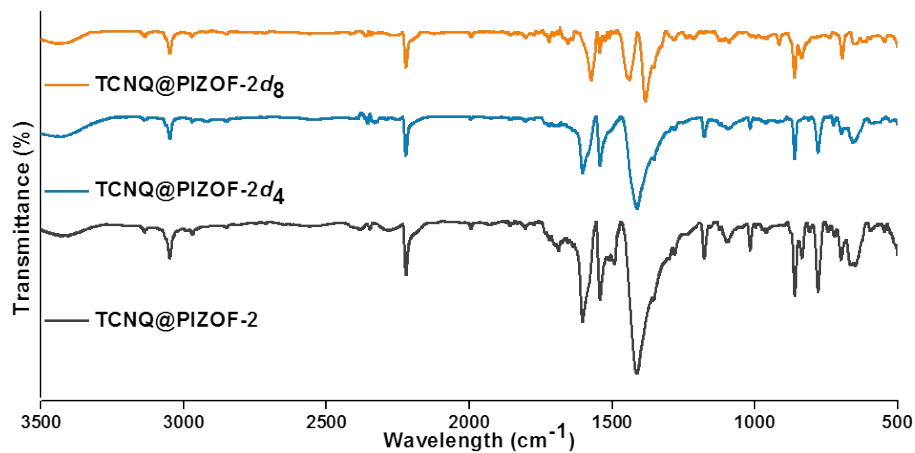


**Figure S10:** IR spectra of the compounds **TCNQ@PIZOF-2d<sub>8</sub>**, **TCNQ@PIZOF-2d<sub>4</sub>** and **TCNQ@PIZOF-2**.

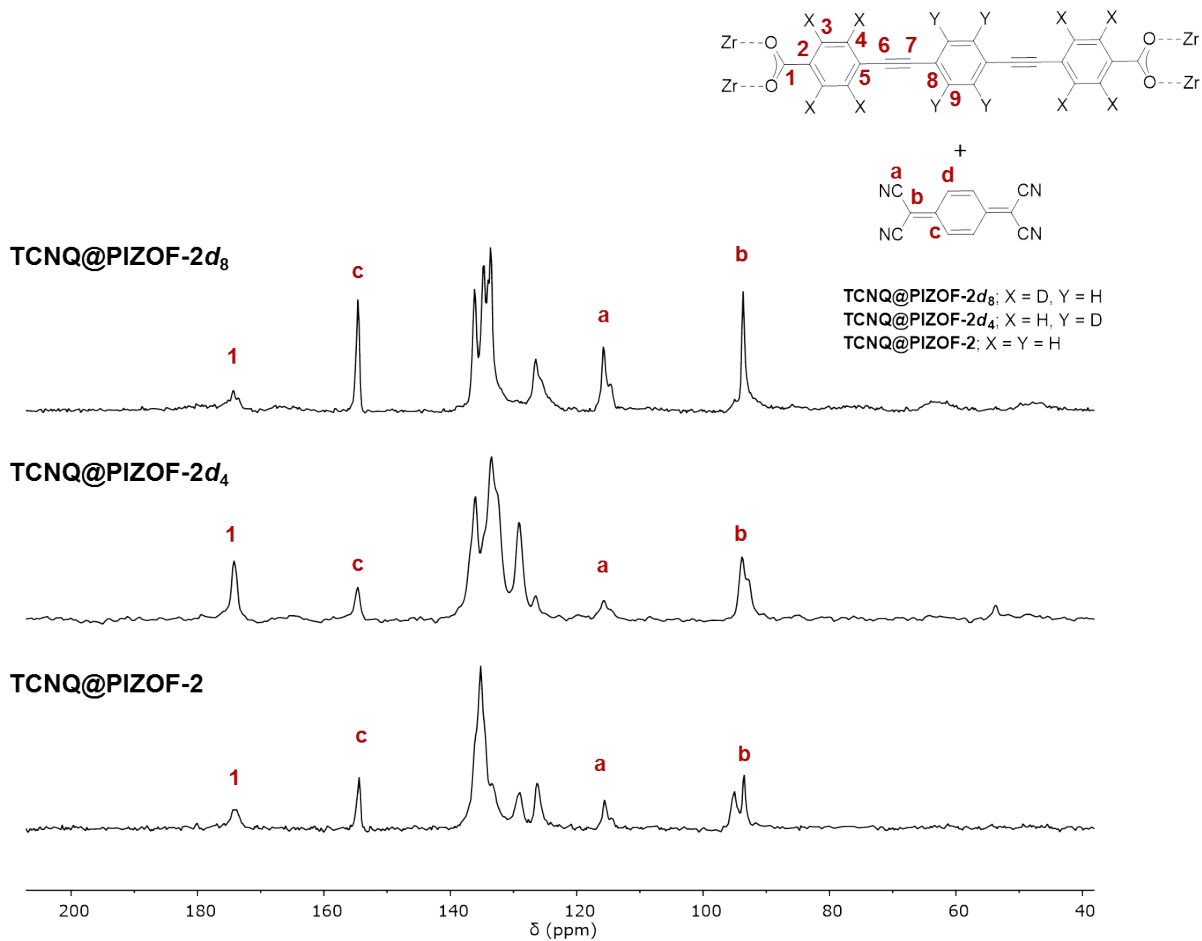


**Figure S11:** Solid state NMR <sup>13</sup>C CPMAS spectra of **TCNQ@PIZOF-2d<sub>8</sub>**, **TCNQ@PIZOF-2d<sub>4</sub>** and **TCNQ@PIZOF-2**.

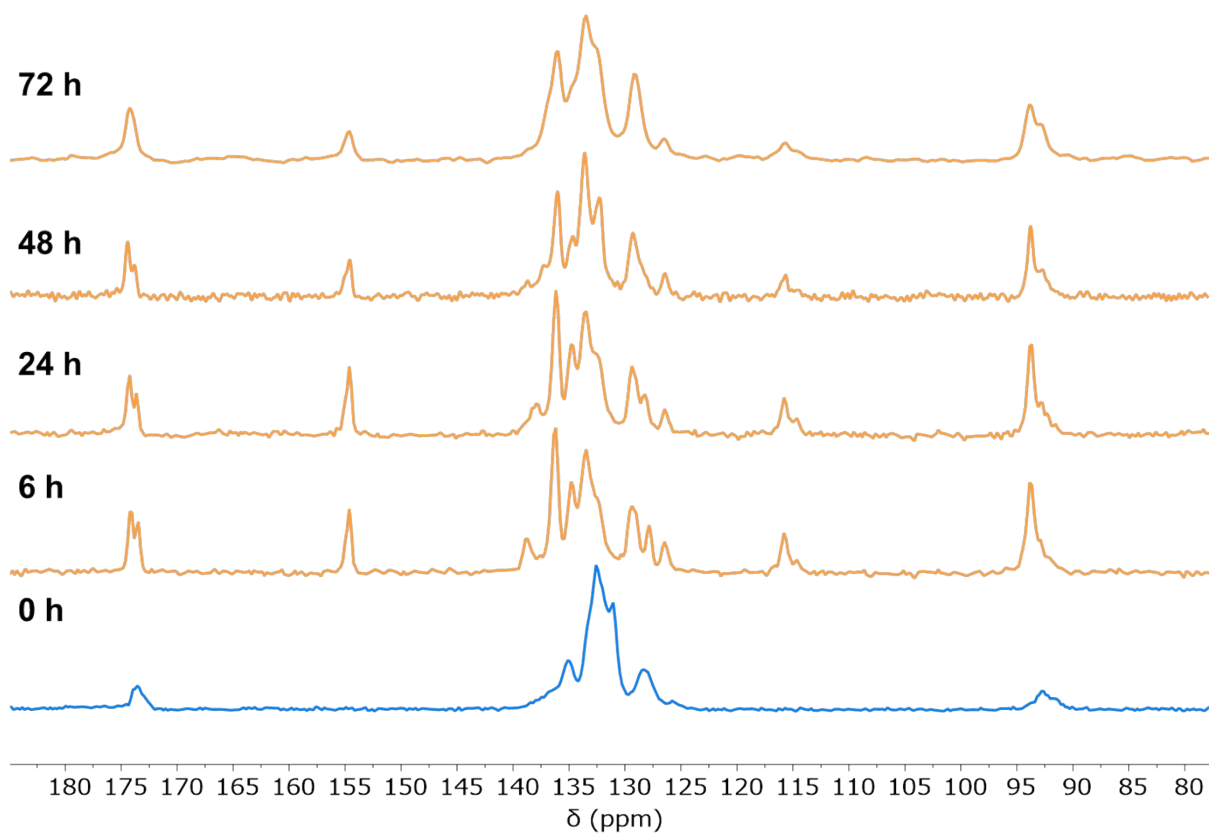


**Figure S12:** Evolution of the  $^{13}\text{C}$  CPMAS spectra in **TCNQ@PIZO-2d<sub>4</sub>** with different infiltration times.

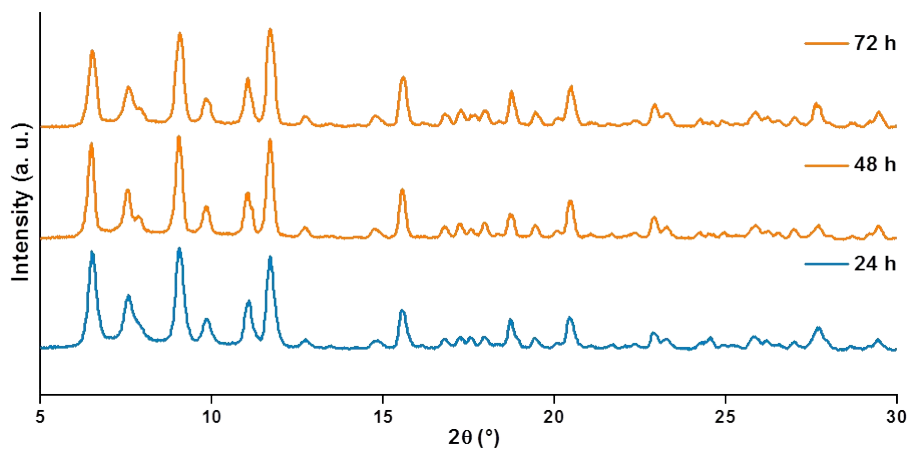


**Figure S13:** PXRD diffraction patterns of **TCNQ@PIZO-2d<sub>4</sub>** varying the infiltration times.

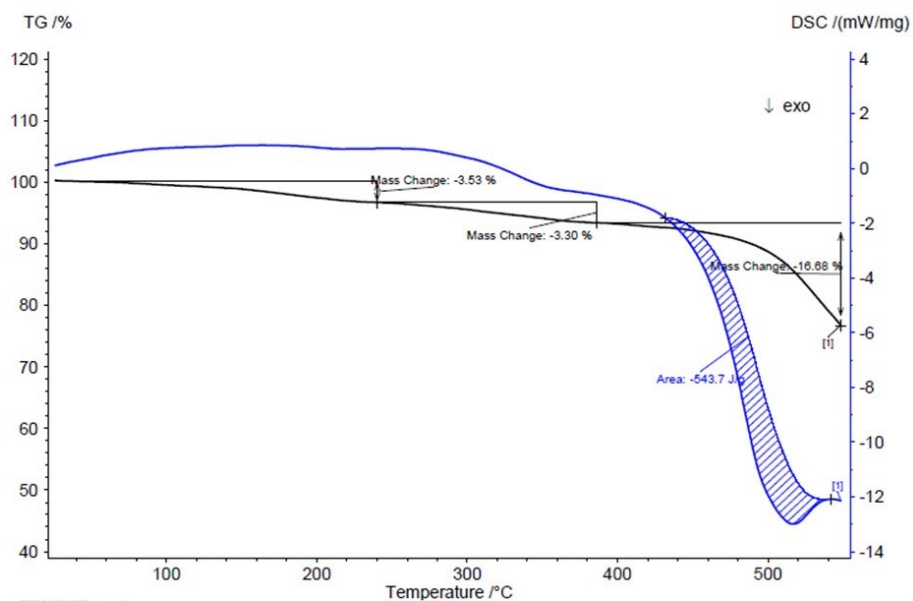


**Figure S14:** Differential scanning calorimetry (blue line) and thermogravimetric analyses (black line) trace of compound **PIZOF-2**.

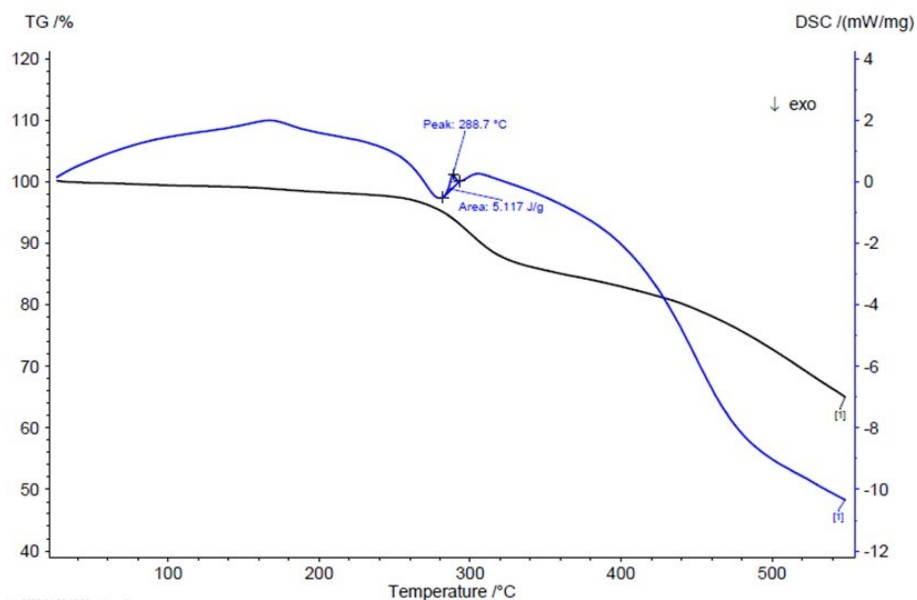


**Figure S15:** Differential scanning calorimetry (blue line) and thermogravimetric analyses (black line) trace of compound **TCNQ@PIZOF-2**.

## 2.4 Determination of TCNQ loaded into MOF samples

TCNQ@PIZOF-2d<sub>4</sub> (15 mg) in CH<sub>2</sub>Cl<sub>2</sub> (10 ml) was added to a 20 mL capped vial and left to stand for 24 hours at room temperature. The suspension was filtered and the residual solution was again graduated to 10 ml using a volumetric flask. The concentration of an aliquot was determined by UV-vis spectroscopy using a calibration plot of absorbance ( $\lambda_{\text{max}} = 400 \text{ nm}$ ) versus TCNQ concentration in the range from 0.5 mM to 2.5 mM.

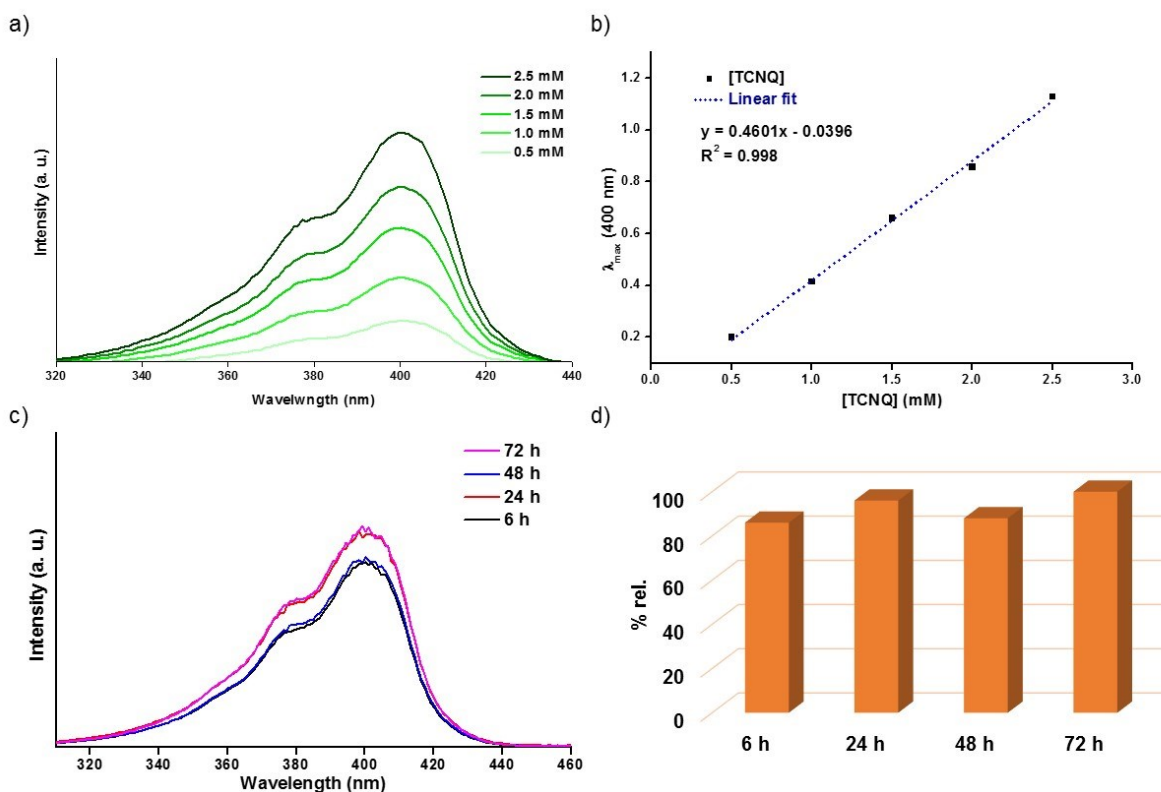


**Figure S16:** a) UV-vis spectra of TCNQ with different concentrations in the range from 0.5 mM to 2.5 mM. b) Calibration plot of the absorbance ( $\lambda_{\text{max}} = 400 \text{ nm}$ ) vs TCNQ concentration with a linear fit (blue line). c) UV-vis spectra of TCNQ@PIZOF-2d<sub>4</sub> with infiltration times of 6 h, 24 h, 48 h, and 72 h. d) Relative concentration plot of TCNQ loaded into PIZOF-2d<sub>4</sub> (Taking as 100 % the intensity of the absorbance at 400 nm of the sample with an infiltration time of 72 h).

**Table S2:** Relevant parameter of the TCNQ concentration loaded into **PIZOF-2d<sub>4</sub>** to afford the compound **TCNQ@PIZOF-2d<sub>4</sub>**. For these calculations, we utilized the molar mass of a deuterated unit cell of MOF  $M_{UnitCell} = 23,467 \text{ g mol}^{-1}$

Infiltration time (h)	PIZOF-2d <sub>4</sub> (mg)	PIZOF-2d <sub>4</sub> (μmol)	TCNQ loaded (mg)	TCNQ (mmol)	Loading TCNQ/PIZOF-2d <sub>4</sub> (molecules per unit cell)	Loading TCNQ/PIZOF-2d <sub>4</sub> (mg/mg)
6	150	$6.39 \times 10^{-3}$	$31.7 \pm 0.6$	$0.155 \pm 0.003$	$24.2 \pm 0.4$	$0.211 \pm 0.4$
24	150	$6.39 \times 10^{-3}$	$37.5 \pm 0.8$	$0.184 \pm 0.004$	$28.8 \pm 0.6$	$0.250 \pm 0.5$
48	150	$6.39 \times 10^{-3}$	$33.1 \pm 0.3$	$0.162 \pm 0.002$	$25.3 \pm 0.3$	$0.221 \pm 0.2$
72	150	$6.39 \times 10^{-3}$	$37.3 \pm 0.3$	$0.183 \pm 0.001$	$28.6 \pm 0.2$	$0.249 \pm 0.2$

## 2.5 <sup>1</sup>H NMR and solid-state NMR <sup>13</sup>C CP MAS spectra

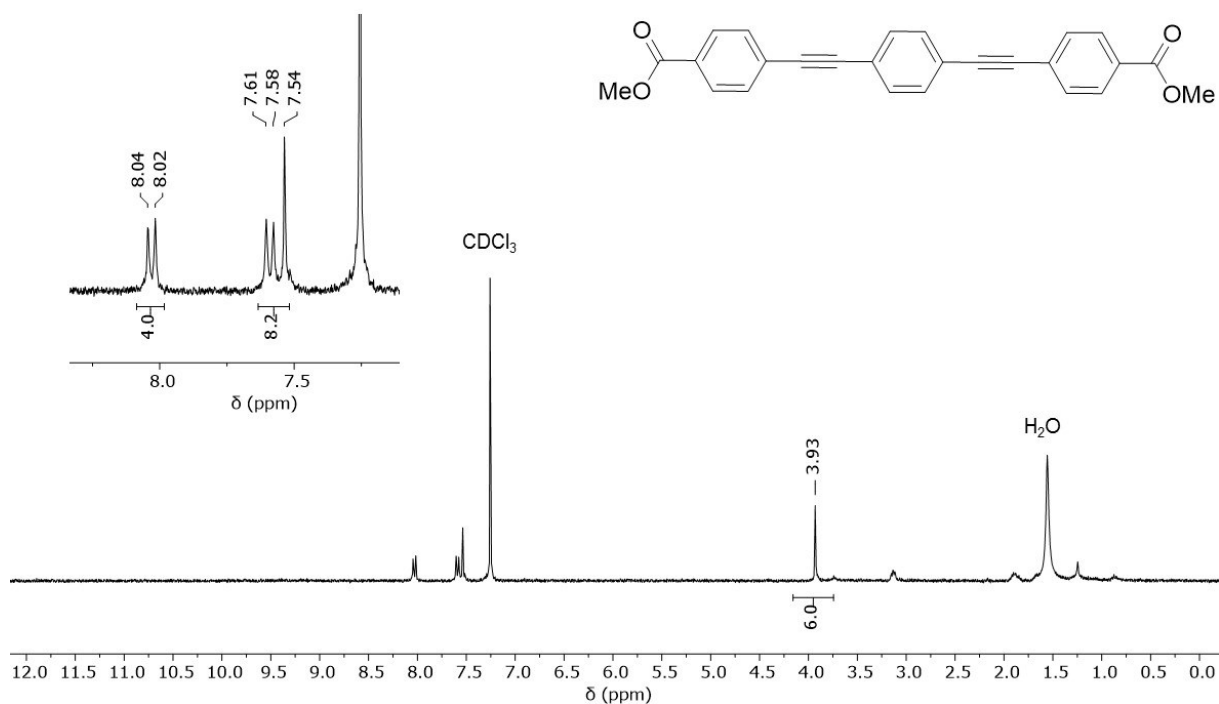


**Figure S17:** <sup>1</sup>H NMR spectrum of compound **Me-PEPEP** (300 MHz, CDCl<sub>3</sub>).

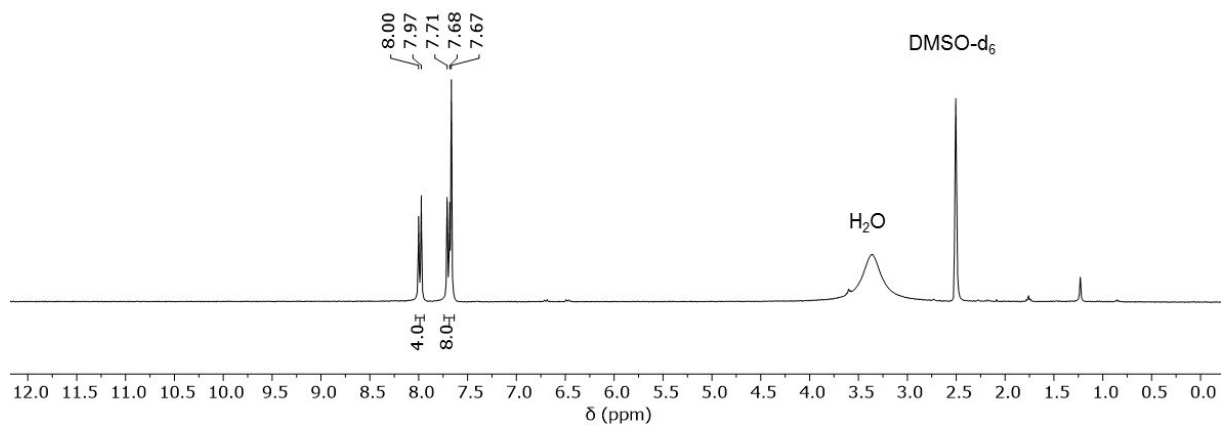
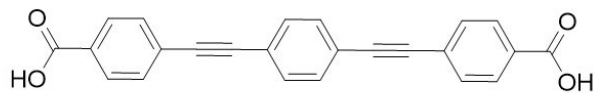


**Figure S18:** <sup>1</sup>H NMR spectrum of compound **PEPEP** (300 MHz, DMSO-d<sub>6</sub>).

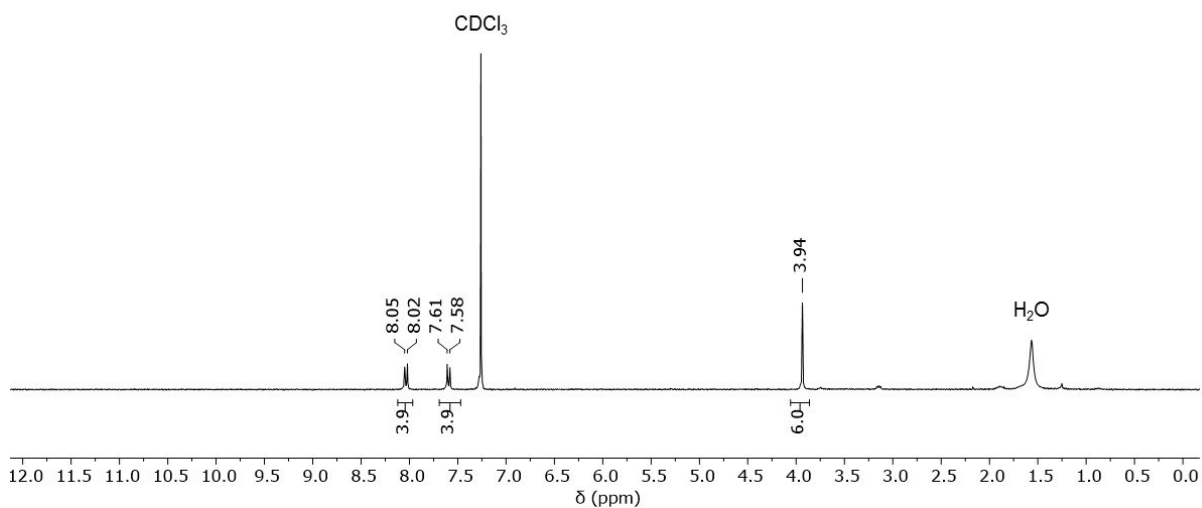
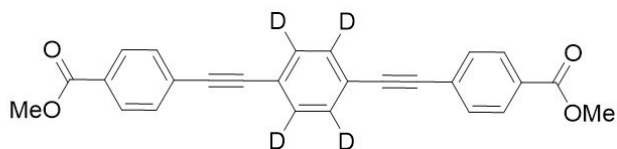


**Figure S19:** <sup>1</sup>H NMR spectrum of compound **Me-PEPEP-d<sub>4</sub>** (300 MHz, CDCl<sub>3</sub>).

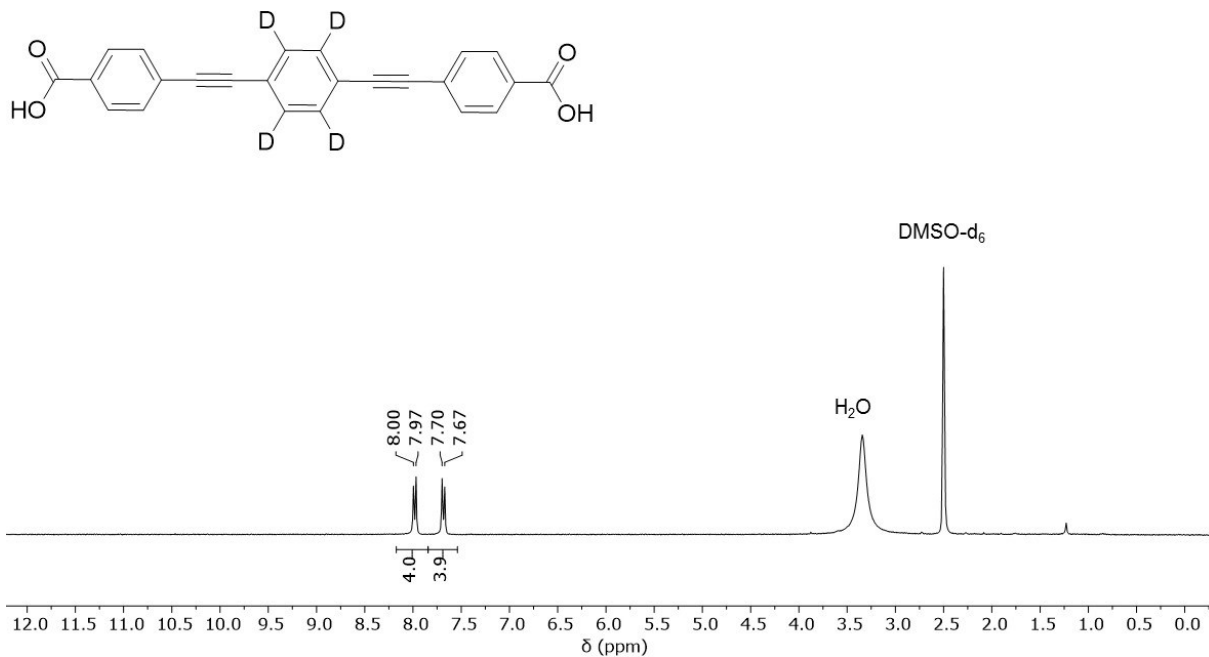


**Figure S20:** <sup>1</sup>H NMR spectrum of compound **PEPEP-*d*<sub>4</sub>** (300 MHz, DMSO-*d*<sub>6</sub>).

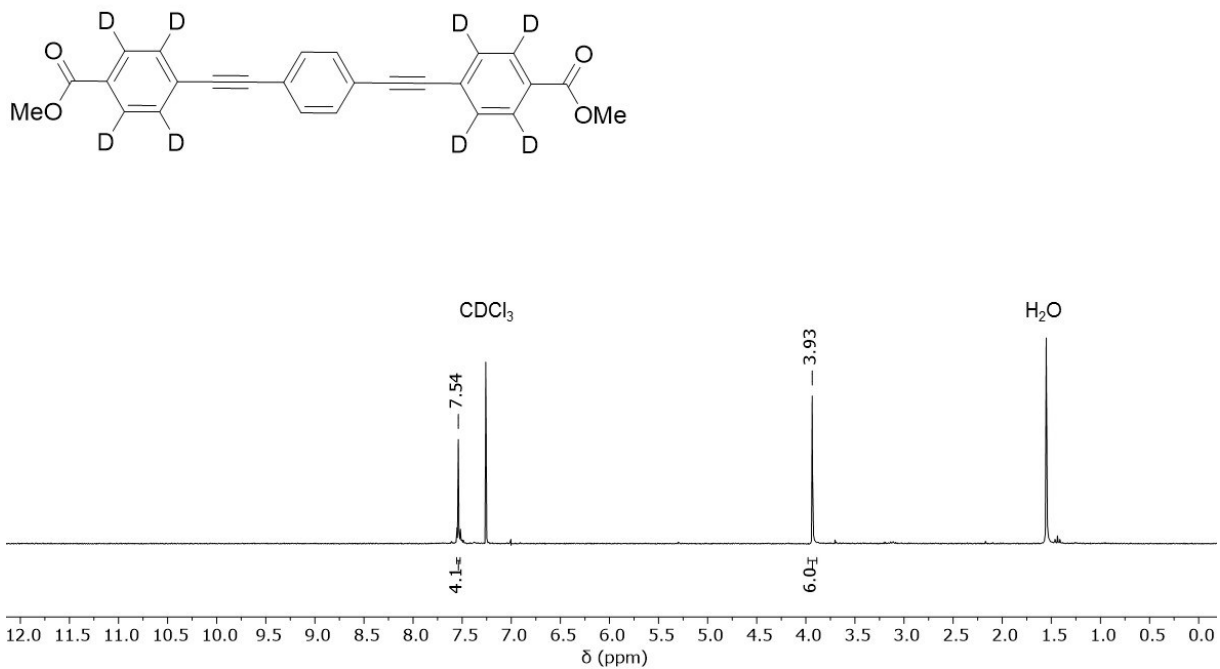


**Figure S21:** <sup>1</sup>H NMR spectrum of compound **Me-PEPEP-*d*<sub>8</sub>** (300 MHz, CDCl<sub>3</sub>).

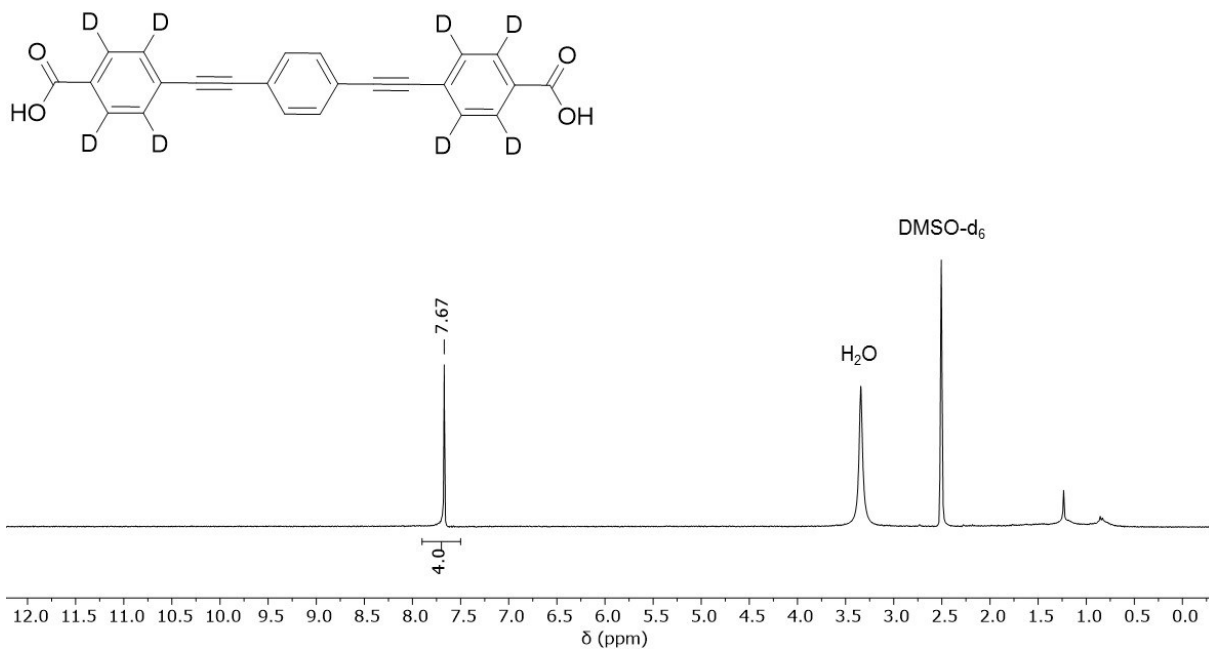


**Figure S22:** <sup>1</sup>H NMR spectrum of compound PEPEP-*d*<sub>8</sub> (300 MHz, DMSO-*d*<sub>6</sub>).

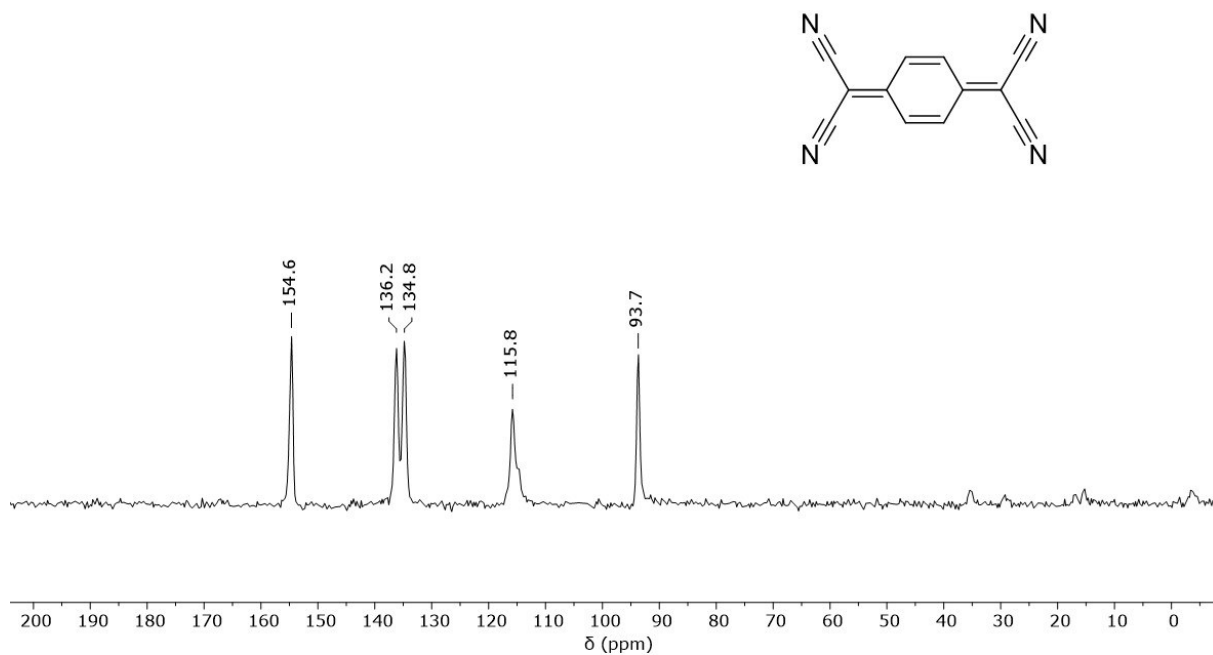


**Figure S23:** Solid-state NMR <sup>13</sup>C CPMAS spectrum of TCNQ.

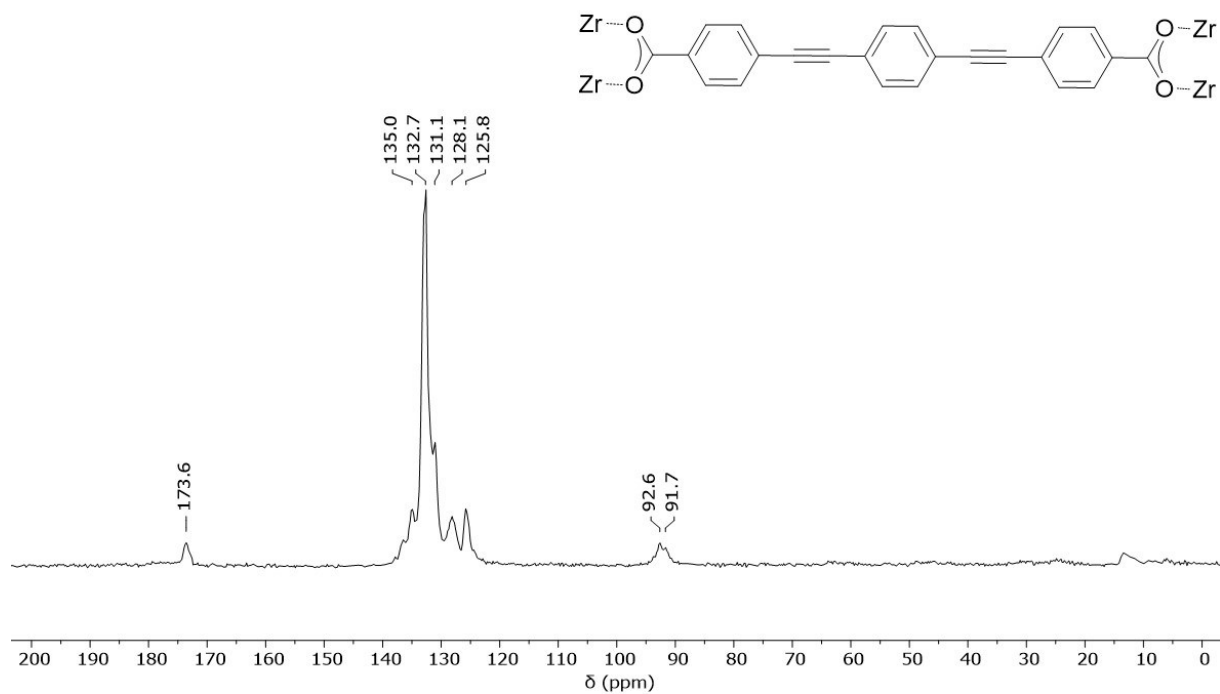


**Figure S24:** Solid-state NMR  $^{13}\text{C}$  CPMAS spectrum of **PIZOF-2**.

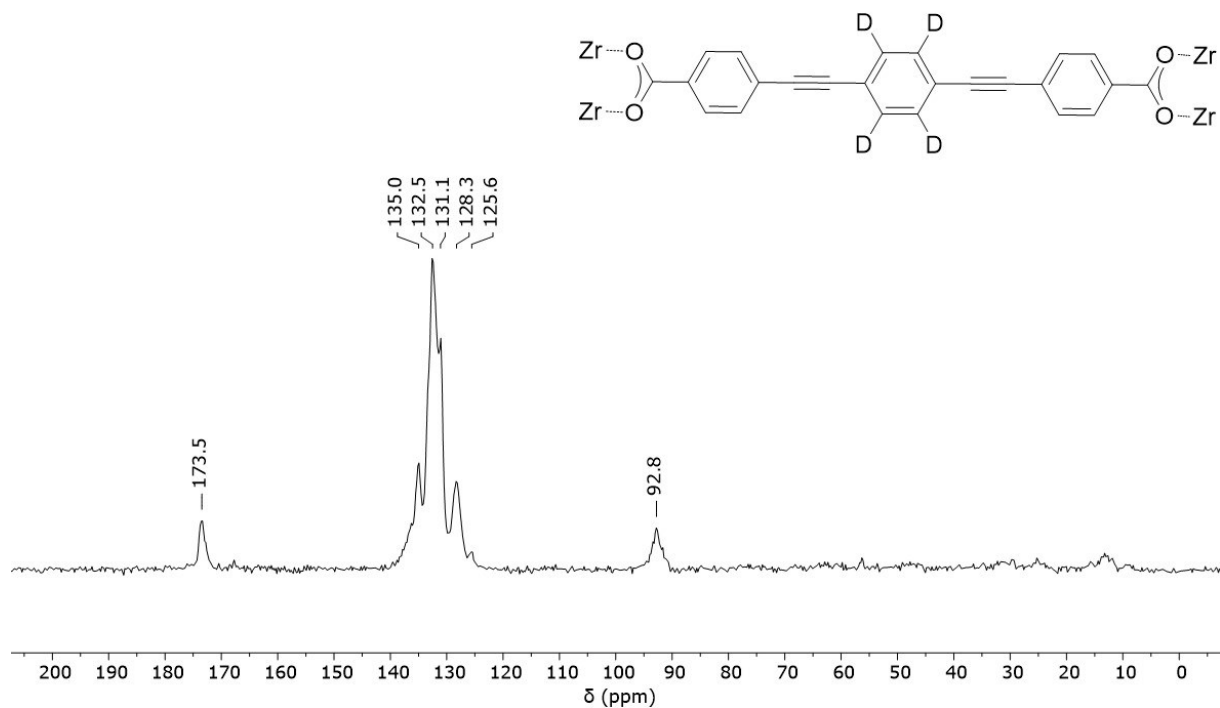


**Figure S25:** Solid-state NMR  $^{13}\text{C}$  CPMAS spectrum of **PIZOF-2d<sub>4</sub>**.

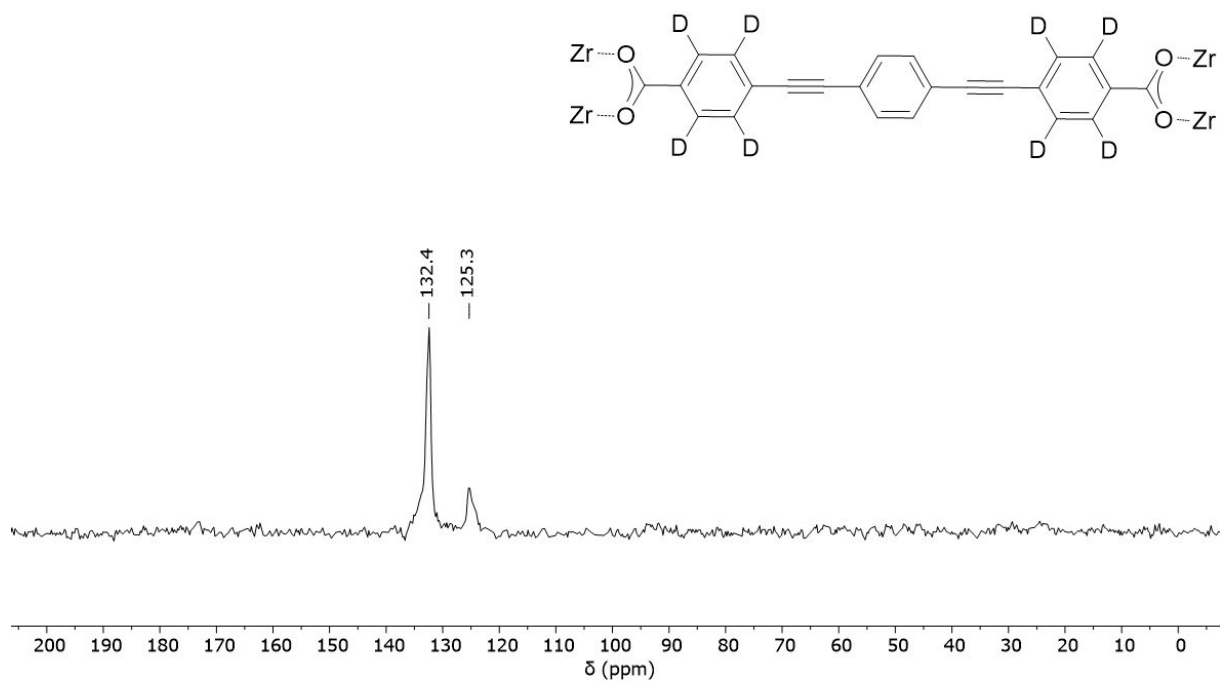


**Figure S26:** Solid-state NMR <sup>13</sup>C CPMAS spectrum of **PIZOF-2d<sub>8</sub>**.

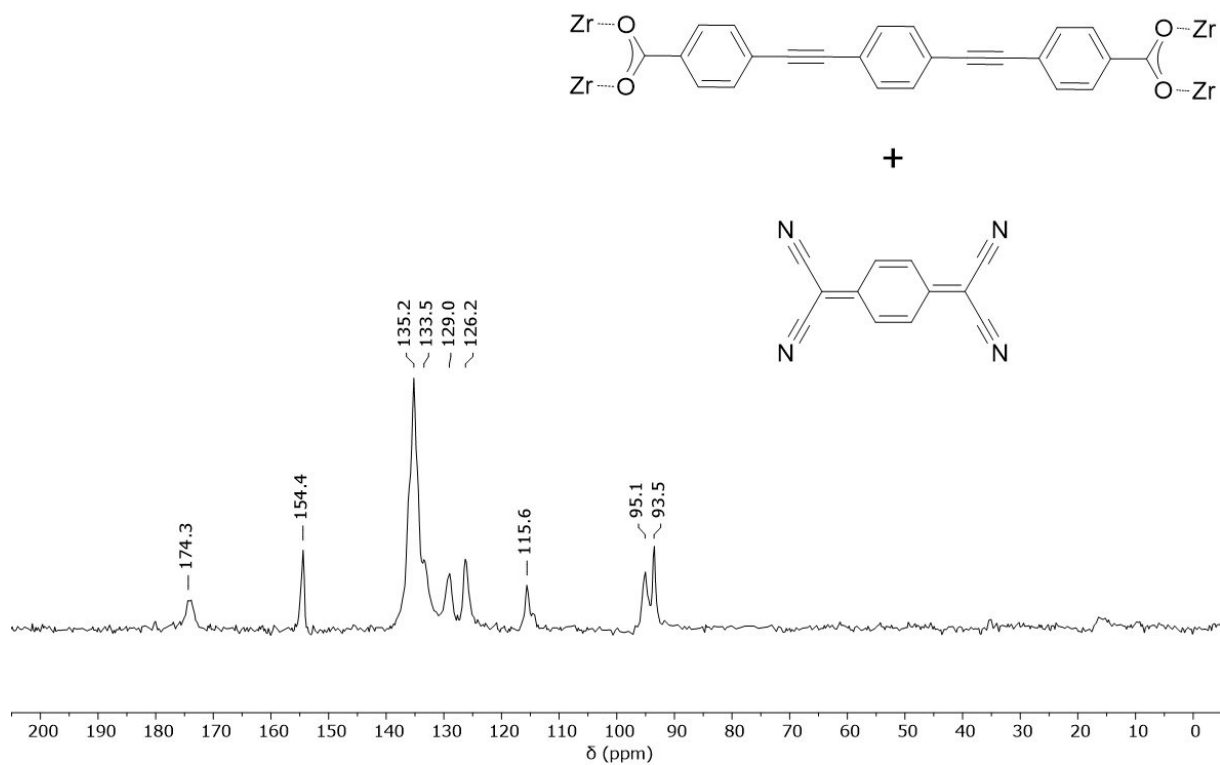


**Figure S27:** Solid-state NMR <sup>13</sup>C CPMAS spectrum of **TCNQ@PIZOF-2**.

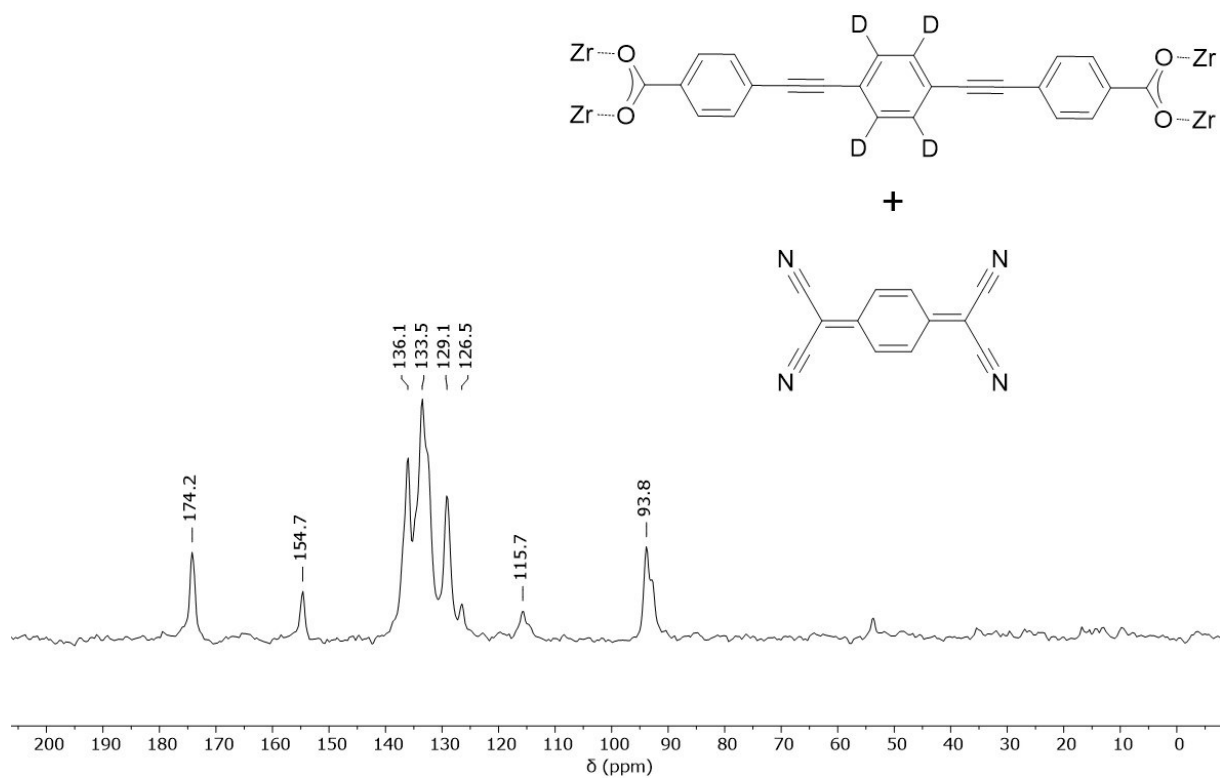


**Figure S28:** Solid-state NMR <sup>13</sup>C CPMAS spectrum of TCNQ@PIZO-2d<sub>4</sub>.

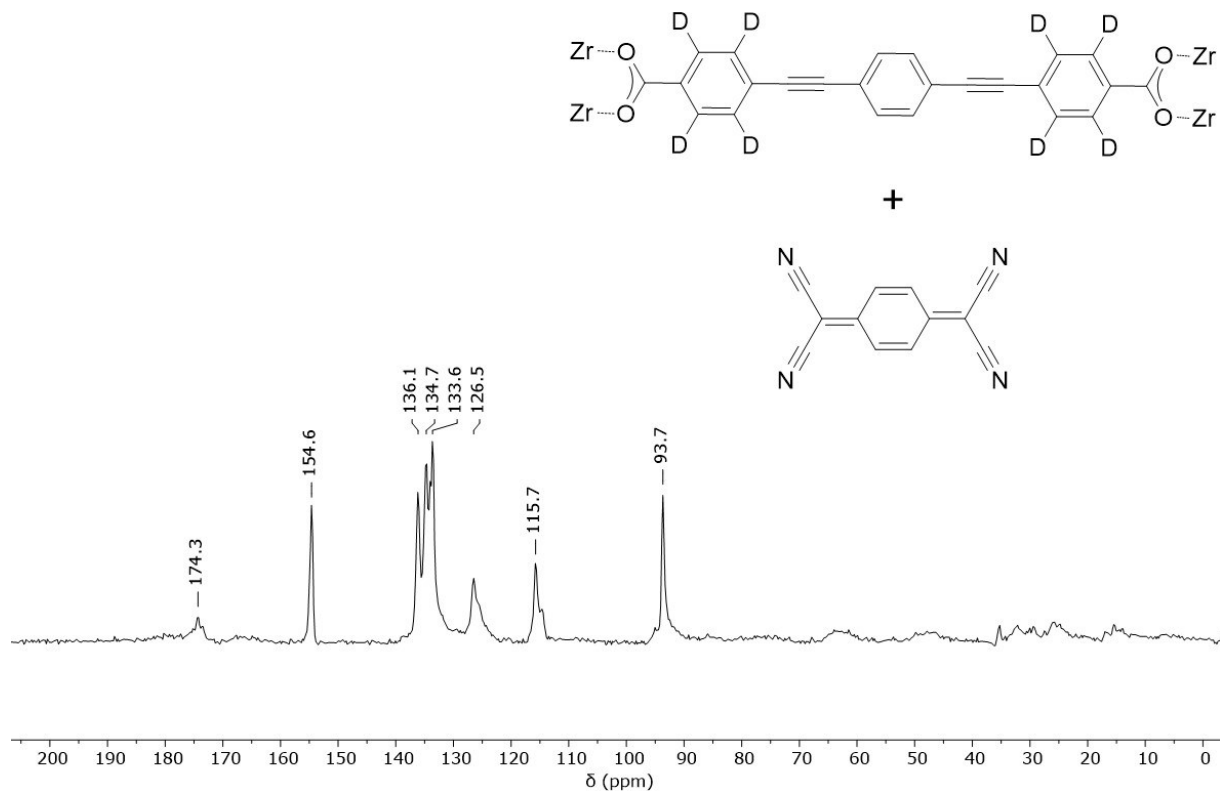


**Figure S29:** Solid-state NMR <sup>13</sup>C CPMAS spectrum of TCNQ@PIZO-2d<sub>8</sub>.

- 
- S1. Macho, V.; Brombacher, L. Spiess, H. W. *Appl. Magn. Reson.*, **2001**, *20*, 405-432.
- S2. Toby, B. H., Von Dreele, R. B. *J. Appl. Crystallogr.*, **2013**, *46*, 544-549.
- S3. Babarao, R.; Rubio-Martínez, M.; Hill, M. R.; Thornton, A. W. *J. Phys. Chem. C* **2016**, *120*, 13013–13023.
- S4. (a) Sonogashira, Y.; Tohda, Y.; Hagihara, N. *Tetrahedron Lett.* **1975**, *50*, 4467–4470.  
(b) Huang, Y.; He, Z. *ACS Catal.* **2016**, *6*, 7814–7823.
- S5. Marshall, R. J.; Griffin, S. L.; Wilson, C.; Forgan, R. S. *Chem. Eur. J.* **2016**, *22*, 4870–4877.
- S6. Doan, T. L. H.; Nguyen, H. L.; Pham, H. Q.; Pham-Tran, N.-N.; Le, T. N.; Cordova, K. E. *Chem. Asian J.* **2015**, *10*, 2660–2668.